

# Differential drag spacecraft rendezvous using an adaptive Lyapunov control strategy

David Pérez<sup>a,\*</sup>, Riccardo Bevilacqua<sup>b</sup>

<sup>a</sup> Mechanical, Aerospace and Nuclear Engineering Department, Rensselaer Polytechnic Institute, JEC 1034 110 8th Street Troy, NY 12180, USA

<sup>b</sup> Mechanical, Aerospace and Nuclear Engineering Department, Rensselaer Polytechnic Institute, JEC 5048 110 8th Street Troy, NY 12180, USA

## ARTICLE INFO

### Article history:

Received 3 May 2012

Received in revised form

28 August 2012

Accepted 15 September 2012

### Keywords:

Differential drag

Adaptive Lyapunov control

## ABSTRACT

This paper introduces a novel Lyapunov-based adaptive control strategy for spacecraft maneuvers using atmospheric differential drag. The control forces required for rendezvous maneuvers at low Earth orbits can be generated by varying the aerodynamic drag affecting each spacecraft. This can be accomplished, for example, by rotating dedicated sets of drag panels. Thus, the relative spacecraft motion can be controlled without using any propellant since the motion of the panels can be powered by solar energy. A novel adaptive Lyapunov controller is designed, and a critical value for the relative drag acceleration that ensures Lyapunov stability is found. The critical value is used to adapt the Lyapunov controller, enhancing its performance. The method is validated using simulations. The results show that the Adaptive Lyapunov technique outperforms previous control strategies for differential drag based spacecraft maneuvering.

© 2012 Elsevier Ltd. All rights reserved.

## 1. Introduction

This paper presents a novel adaptive Lyapunov control strategy to perform spacecraft rendezvous maneuvers at low Earth orbits (LEO), exploiting atmospheric differential drag forces. Leonard ([1]) introduced an alternative method for generating the control forces required by the rendezvous maneuvers at LEO. This method consists of varying the aerodynamic drag experienced by different spacecraft, thus generating differential accelerations between them. The interest towards this methodology comes from the decisive role that efficient and autonomous spacecraft rendezvous maneuvering will have in future space missions. In order to increase the efficiency and economic viability of such maneuvers, propellant consumption must be minimized. Employing the differential drag based methodology allows for virtually propellant-free control of the relative orbits, since maneuverable dedicated drag surfaces can be powered

by solar energy. The ORBCOMM constellation formation keeping ([2]) is the first application of these ideas, while, the JC2Sat project developed by the Canadian and Japanese Space Agencies ([3–5]) is an envisioned application of these ideas. Moreover, control of space rendezvous maneuvers is an increasingly important topic given the potential for its application for on-orbit maintenance missions. NASA targets the development of such missions through its Satellite Servicing Capabilities Office ([6]).

The variation in the drag can be induced, for example, by closing or opening flat panels attached to the spacecraft, hence effectively modifying its ballistic coefficient. The reference frame commonly employed for spacecraft relative motion representation is the local vertical local horizontal (LVLH) reference frame, where  $x$  points from Earth to the reference satellite (virtual or real),  $y$  points along the track (direction of motion), and  $z$  completes the right-handed frame (see Fig. 1). In such a frame, a target and a chaser spacecraft are envisioned, and the following three cases for the configurations of the panels are considered (see Fig. 1):

1. All the panels of the chaser are deployed generating the maximum possible drag while those of the target

\* Corresponding author. Tel.: +1 518 276 3191;

fax: +1 518 276 2623.

E-mail addresses: [perezd3@rpi.edu](mailto:perezd3@rpi.edu) (D. Pérez), [bevilr@rpi.edu](mailto:bevilr@rpi.edu) (R. Bevilacqua).

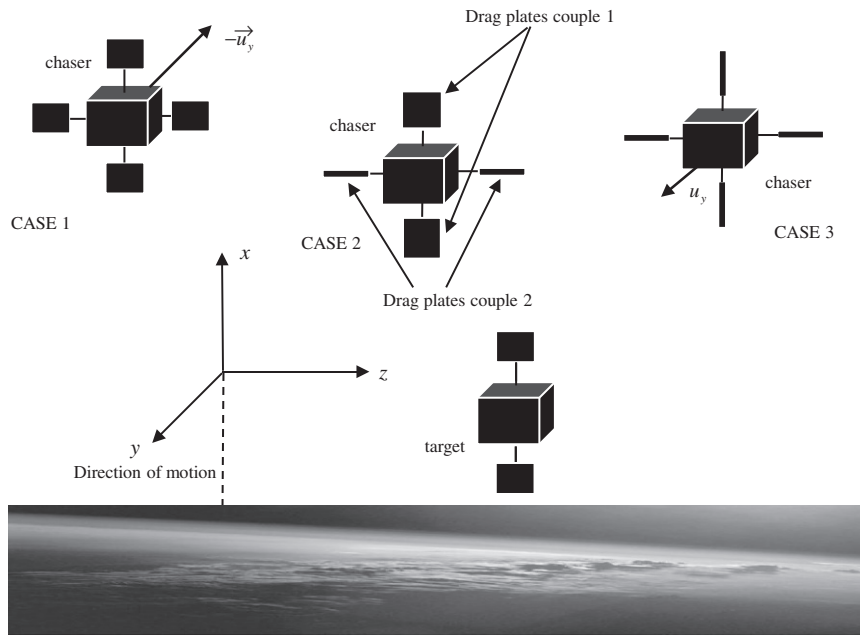


Fig. 1. Drag panels concept to generate differential drag (adapted from Ref. [7]).

are not deployed to achieve the opposite, hence generating a negative acceleration of the chaser relative to the target.

2. All the panels of the target are deployed generating the maximum possible drag while those of the chaser are not deployed to achieve the opposite, thus generating a positive acceleration of the chaser relative to the target.
3. Both chaser and target have a couple of panels deployed, which means that there is no relative acceleration between the spacecraft. This can be also achieved by having both spacecraft closing all of their panels.

Atmospheric differential drag is expected to provide an effective control only in the orbital plane ( $x$  and  $y$ ); for this reason we will limit our discussions to the in-plane motion, assuming that no out-of-plane ( $z$ ) motion is present, or that it is controlled with different means.

The magnitude of the differential drag acceleration fluctuates during the maneuver as the spacecraft encounters regions of the thermosphere with different atmospheric densities. In the thermosphere, atmospheric density can change significantly due to solar and geomagnetic activities. These variations are difficult to model and measure accurately on board; hence, robust control strategies must be designed to increase the reliability of spacecraft maneuvering using differential drag.

The problem of designing a control system for the rendezvous maneuver using differential drag becomes the problem of designing a real-time logic to command the closed and open positions for the flat panels, with the intent of forcing the satellites to follow the desired rendezvous trajectory, or simply regulate to a final

desired state (rendezvous). The sought-for logic needs to be based on the assumption that the control is either positive maximum, negative maximum, or zero (Fig. 1) neglecting the time required by the panels to rotate. This logic is here designed using a Lyapunov approach. In essence, a Lyapunov function of the tracking error is selected, and the control signal is chosen so that the tracking error converges to zero (i.e., the first order time derivative of the Lyapunov function is negative), thus, the nonlinear dynamics of the system are forced to follow a desired trajectory. This significantly simplifies the control problem, since the desired trajectory can be designed using controlled linear dynamics approximating the reality of spacecraft relative motion. The method proposed here builds upon and improves previous work presented and tested in Refs. [7–9].

In particular, a stable linear reference model is introduced; this model tracks the desired rendezvous trajectory. The Lyapunov controller can then be used to either directly track the desired trajectory or track the dynamics of the linear reference model. In this work the Lyapunov controller is directly tracking the final desired position, that is the zero relative position and velocity between chaser and target spacecraft, which is the rendezvous condition. The stable linear reference model is still needed for the regulation case, even if the linear reference is not tracked. In fact, the linear stable model enables the definition of the correct Lyapunov function that in turns drives the nonlinear dynamics to behave in a desired fashion in terms of time response.

In order to enhance the performance and robustness of the Lyapunov controller, a way of adapting the Lyapunov function, in terms of the drag acceleration critical value necessary for stability, is developed. The definition of

appropriate Lyapunov functions is a challenge that varies from problem to problem, and a widely studied theory exists ([10–12]). In this work, we define a quadratic Lyapunov function of the tracking error, and we change its positive definite matrix in an adaptive fashion, effectively changing the Lyapunov function in real time to achieve the best performances during the rendezvous maneuvers. The adaptation is achieved through analytical expressions giving the dependence of the differential drag acceleration critical value from the chosen stable linear model. By means of these relationships, the differential drag critical value is maintained minimal during the maneuver, achieving the best possible control authority margin in real time. All the derivatives necessary to obtain the analytical results are computed and presented in the paper.

The foremost contributions of this work are:

- 1) An analytical expression, for the differential drag acceleration critical value, that ensures stability in the sense of Lyapunov for the system.
- 2) Analytical expressions for the partial derivatives of the critical value of the differential drag acceleration in terms of  $\underline{Q}$  (Lyapunov equation matrix), and  $\underline{A}_d$  (reference linear dynamics matrix).
- 3) A control strategy, based on the Lyapunov approach, for two spacecraft rendezvous using differential drag, which uses adaptation to choose in real time an appropriate positive definite matrix  $\underline{P}$  in a quadratic Lyapunov function.
- 4) Demonstration of feasibility of the approach via Satellite Tool Kit (STK) numerical simulations.
- 5) Assessment of the performances of the designed adaptive Lyapunov control strategy in terms of the duration of the rendezvous maneuver and the number of switches in the differential drag (control effort), in comparison with the non adaptive Lyapunov control strategy previously presented by the authors in Ref. [9].
- 6) Overall, this paper provides a valuable strategy that can be implemented onboard real spacecraft, even small spacecraft with limited computing capabilities. In fact, the adaptive Lyapunov-based control methodology does not require numerical iterations and can run in real time, requiring onboard measurements that would be available during flight.

The paper is organized as follows. Section 2 introduces the concept of atmospheric differential drag and its mathematical expression. Section 3 illustrates the spacecraft relative motion linear and nonlinear dynamics employed in the following developments. Section 4 is dedicated to the Lyapunov function definition, the panels' activation strategy, as well as the analytical derivatives of the differential drag critical value with respect to the independent variable matrices. In Section 5 such derivatives are used to create the novel adaptive Lyapunov controller. Section 6 validates the approach via Satellite Tool Kit numerical simulations, and Section 7 draws the conclusions.

## 2. Differential drag

The drag acceleration experienced by spacecraft at LEO is a function of the atmospheric density, atmospheric winds, velocity of the spacecraft relative to the medium, and the geometry, attitude, drag coefficient and mass of the spacecraft. The interdependence of these parameters (e.g., the drag coefficient is affected by the temperature of the medium which also determines the density of the medium) and the lack of knowledge in some of their dynamics make the modeling of the drag force a challenging and still largely unsolved problem. This results in large uncertainties regarding the control forces available for maneuvers using drag forces. Consequently the control systems used for drag maneuvers must be able to cope with these uncertainties.

The aerodynamic acceleration experienced by a spacecraft is typically decomposed into the lift (lift forces are negligible at LEO) and drag forces, the latter usually expressed as:

$$a_d = \frac{1}{2}\rho BC v_s^2 \quad (1)$$

where  $\rho$  is the atmospheric density,  $v_s$  is the velocity of the spacecraft relative to the atmospheric particles. The ballistic coefficient  $BC$  is given by:

$$BC = \frac{C_D A}{m} \quad (2)$$

where  $C_D$  is the drag coefficient of the spacecraft,  $A$  is the cross-wind surface area of the spacecraft and  $m$  is the mass of the spacecraft.

Using Eq. (1), the magnitude of the relative acceleration caused by the differential aerodynamic drag for the spacecraft system (target and chaser) is given as:

$$a_{Drel} = \frac{1}{2}\rho \Delta BC v_s^2 \quad (3)$$

where  $\Delta BC$  is the difference in ballistic coefficients between the target and chaser. See Fig. 1.

In the thermosphere, the solar activity creates large variations of temperature, which drive variations of the atmospheric density. These variations produce significant changes in the available magnitude of drag acceleration for a given ballistic coefficient.

## 3. Linear reference and nonlinear models

Hill's groundbreaking work on lunar motion ([13]), which described the motion of the Moon relative to the Earth, was the first study on the relative motion of bodies in space. Afterwards, inspired by Hill's work, Clohessy and Wiltshire ([14]) developed a linear model, which describes the motion of a chaser spacecraft relative to a target spacecraft. This model has been widely used in applications involving low thrust proximity maneuvers. Unfortunately, this model does not account for the differential effects on the spacecraft motion due to nonlinearities such as the  $J_2$  perturbation, caused by the Earth's flattening. The effect of the  $J_2$  perturbation and other nonlinearities is more significant in maneuvers with longer times of execution such as those performed using differential drag. For this reason the use of a linear model

that partially accounts for averaged effects of these nonlinearities is desired, as the one described in the following section. The model described in the following section is used for the derivation of the Lyapunov controller.

### 3.1. Linear reference model

A linearized model which represents the relative motion of spacecraft under the influence of  $J_2$  was developed by Schweighart and Sedwick ([15]). Adding the control acceleration vector ( $\mathbf{u}$ ) to the Schweighart and Sedwick equations, the following system of linear differential equations in the LVLH frame is obtained.

$$\dot{\mathbf{x}}_d = \mathbf{A}\mathbf{x}_d + \mathbf{B}\mathbf{u}, \quad \mathbf{A} = \begin{bmatrix} \mathbf{0}_{2 \times 2} & \mathbf{I}_{2 \times 2} \\ b & 0 & 0 & a \\ 0 & 0 & -a & 0 \end{bmatrix}, \quad \mathbf{B} = \begin{bmatrix} 0 \\ 0 \\ 0 \\ 1 \end{bmatrix},$$

$$\mathbf{x}_d = \begin{bmatrix} x_d \\ y_d \\ \dot{x}_d \\ \dot{y}_d \end{bmatrix}, \quad a = 2nc, \quad b = (5c^2 - 2)n^2,$$

$$c = \sqrt{1 + \frac{3J_2 R}{8r_t^2} [1 + 3 \cos(2i_t)]}, \quad d = \sqrt{a^2 - b} \quad (4)$$

where  $n$  is the mean motion of the target,  $J_2$  is the second zonal harmonic,  $R$  is the Earth mean radius,  $r_t$  is the target's orbit radius and  $i_t$  is the target's inclination. The control action is only along the  $y$  direction, see Fig. 1.

Since the dynamics of the Schweighart and Sedwick model are unstable, a linear quadratic regulator (LQR) feedback controller is used to stabilize them and obtain the necessary linear model for Lyapunov developments. The resulting reference model is described by:

$$\dot{\mathbf{x}}_d = \mathbf{A}_d \mathbf{x}_d + \mathbf{B}_d \mathbf{u}_d, \quad \mathbf{A}_d = \mathbf{A} - \mathbf{B}\mathbf{K}, \quad \mathbf{u}_d = \mathbf{K}\mathbf{x}_t \quad (5)$$

where  $\mathbf{K}$  is a constant matrix found by solving the LQR problem for the Schweighart and Sedwick model, thus ensuring  $\mathbf{A}_d$  to be Hurwitz, and  $\mathbf{x}_t$  is the desired guidance. The  $\mathbf{Q}_{LQR}$  matrix and  $R_{LQR}$  value used to solve the LQR problem are:

$$\mathbf{Q}_{LQR} = \mathbf{I}_{4 \times 4}, \quad R_{LQR} = 1.5 \times 10^{18} \quad (6)$$

The state vector  $\mathbf{x}_d$  is the desired reference trajectory, and control action is along the  $y$  direction only (since the drag force acts always opposite to the direction of motion). This stable linear reference system can be regulated or forced to track a desired guidance trajectory.

### 3.2. Nonlinear model

The dynamics of spacecraft relative motion are nonlinear due to effects such as the  $J_2$  perturbation, and the nonlinear variations on the atmospheric density at LEO. The adaptive Lyapunov-based approach suggested here intends to cope with these unmodeled effects, by minimizing the differential drag critical value at all times. In this section the model that will be used for the nonlinear dynamics is presented. The general expression for the real world nonlinear dynamics, including nonlinearities such as

the  $J_2$  perturbation, is defined as:

$$\dot{\mathbf{x}} = \mathbf{f}(\mathbf{x}) + \mathbf{B}\mathbf{u}, \quad \mathbf{x} = [x \ y \ \dot{x} \ \dot{y}]^T, \quad \mathbf{u} = \begin{cases} a_{Drel} \\ 0 \\ -a_{Drel} \end{cases} \quad (7)$$

where  $a_{Drel}$  acts along the  $y$  direction only, as explained earlier. All the nonlinearities are accounted for in the nonlinear function  $\mathbf{f}(\mathbf{x})$ . For the development of the Lyapunov controller  $\mathbf{f}(\mathbf{x})$  is assumed to be a function of the spacecraft position only, and is assumed (for a single spacecraft in the inertial frame) to be:

$$\mathbf{f}(\mathbf{r}) = \frac{-\mu \mathbf{r}}{r^3}, \quad \mathbf{r} = [x_{in} \ y_{in} \ z_{in}]^T \quad (8)$$

where  $\mathbf{r}$  is the position vector of the spacecraft in the inertial frame,  $r$  is its magnitude and  $\mu$  is the gravitational parameter.

## 4. Lyapunov approach

In this section, the nonlinear adaptive control law based on the Lyapunov approach is described. The approach is inspired by previous work from one of the authors ([8]) and was further developed by the authors in Ref. [9].

A Lyapunov function is defined as:

$$V = \mathbf{e}^T \mathbf{P} \mathbf{e}, \quad \mathbf{e} = \mathbf{x} - \mathbf{x}_d, \quad \dot{\mathbf{e}} = \dot{\mathbf{x}} - \dot{\mathbf{x}}_d \quad (9)$$

where  $\mathbf{P}$  is a positive definite matrix,  $\mathbf{e}$  is the tracking error vector,  $\mathbf{x}$  and  $\mathbf{x}_d$  are defined as the actual spacecraft relative state vector and the reference state vector, respectively. The first order time derivative of the Lyapunov function can be manipulated to obtain:

$$\dot{V} = \mathbf{e}^T (\mathbf{A}_d^T \mathbf{P} + \mathbf{P} \mathbf{A}_d) \mathbf{e} + 2\mathbf{e}^T \mathbf{P} (\mathbf{f}(\mathbf{x}) - \mathbf{A}_d \mathbf{x} + \mathbf{B}_d a_{Drel} \hat{u} - \mathbf{B}_d \mathbf{u}_d). \quad (10)$$

where  $\hat{u}$  is the command sent to the panel actuators. If the matrix  $\mathbf{A}_d$  is Hurwitz, a symmetric positive definite matrix  $\mathbf{Q}$  is chosen such that the Lyapunov equation (11) is satisfied. For this reason the reference model must be stable, which is the case for the stabilized Schweighart and Sedwick model shown in Eq. (5). For a given set of matrices  $\mathbf{Q}$  and  $\mathbf{A}_d$  the following Lyapunov equation must be solved to find  $\mathbf{P}$ .

$$-\mathbf{Q} = \mathbf{A}_d^T \mathbf{P} + \mathbf{P} \mathbf{A}_d \quad (11)$$

Choosing a symmetric positive definite  $\mathbf{Q}$  matrix, results in the following expression for the time derivative of the Lyapunov function:

$$\dot{V} = -\mathbf{e}^T \mathbf{Q} \mathbf{e} + 2\Delta \quad (12)$$

where  $\Delta$  is given by:

$$\Delta = \beta \hat{u} - \delta \quad (13)$$

and  $\beta$ ,  $\delta$  and  $\hat{u}$  are given by the following expressions:

$$\beta = \mathbf{e}^T \mathbf{P} \mathbf{B}_d a_{Drel}, \quad \hat{u} = \begin{cases} 1 \\ 0 \\ -1 \end{cases} \quad (14)$$

$$\delta = \mathbf{e}^T \mathbf{P} (\mathbf{A}_d \mathbf{x} - \mathbf{f}(\mathbf{x}) + \mathbf{B}_d \mathbf{u}_d) \quad (15)$$

The three states for  $\hat{u}$  represent the commands: all panels open on chaser and all closed on target ( $-1$ ), no differential between spacecraft, i.e., same panels deployed or no panels deployed on both spacecraft ( $0$ ), and the opposite of the first configuration, i.e., all panels open on target and all closed on chaser ( $1$ ).

Eqs. (10), (12) and (15) represent the case in which the nonlinear system is tracking the reference model (state vector  $\mathbf{x}$  tracks  $\mathbf{x}_d$ ); however, if the nonlinear system, directly tracks a desired guidance ( $\mathbf{x}_r$ ), Eqs. (10), (12) and (15) simplify to:

$$\dot{V} = 2\mathbf{e}^T \mathbf{P}(\mathbf{f}(\mathbf{x}) - \dot{\mathbf{x}}_r + \mathbf{B}a_{Drel}\hat{u}) = 2\Delta, \quad \delta = \mathbf{e}^T \mathbf{P}(\dot{\mathbf{x}}_r - \mathbf{f}(\mathbf{x})) \quad (16)$$

Furthermore, if the desired guidance is assumed to be a constant zero state vector, (the controller acts as a regulator), which is the desired final state for a rendezvous maneuver (zero relative position and velocity between chaser and target), Eqs. (10), (12) and (15) are reduced to:

$$\dot{V} = 2\mathbf{e}^T \mathbf{P}(\mathbf{f}(\mathbf{x}) + \mathbf{B}a_{Drel}\hat{u}) = 2\Delta, \quad \delta = -\mathbf{e}^T \mathbf{P}\mathbf{f}(\mathbf{x}) \quad (17)$$

It must be mentioned that even though the matrices  $\mathbf{A}_d$  and  $\mathbf{Q}$  are not present in Eqs. (16) and (17), they still affect the behavior of  $\dot{V}$  since they are used to obtain  $\mathbf{P}$ . This causes the matrix  $\mathbf{P}$  to still contain information on the linearized dynamics of the system initially contained in matrix  $\mathbf{A}_d$ . The  $\mathbf{P}$  matrix enforces certain relationships among the system's states, and also weights their contribution within the Lyapunov function, in such a way to obtain a desired controlled relative motion between the two spacecraft. The characteristics of this desired motion (e.g., time response) are chosen by selecting the linear dynamics.

#### 4.1. Drag panels activation strategy

Guaranteeing  $\Delta \leq 0$  would imply that the tracking error ( $\mathbf{e}$ ) converges to zero, since the term involving  $\mathbf{Q}$  is already negative. In other words, as long as  $\Delta \leq 0$ , the system dynamics of the spacecraft will converge to the desired state. However, since the control variable  $\hat{u}$  does not affect  $\delta$ , the system cannot be guaranteed to be Lyapunov stable for the chosen Lyapunov function if  $\delta$  is positive, and has a higher magnitude than  $\beta$ . The magnitude of  $\beta$  is linearly dependent on the atmospheric density  $\rho$ , which indicates that if  $\rho$  is too small the system is unstable since  $\beta$  will not have a magnitude large enough to overcome a positive value of  $\delta$  of greater magnitude. In other words, the motion of the spacecraft cannot be controlled if  $\rho$  is not large enough, that is, there is not enough control authority (not enough drag force for controlling the spacecraft motion).

The activation strategy for the control (as proposed in Ref. [9]) is designed such that the chosen value of  $\hat{u}$  forces the product  $\beta\hat{u}$  to be negative, thus  $\hat{u}$  can be expressed as:

$$\hat{u} = -\text{sign}(\beta) = -\text{sign}(\mathbf{e}^T \mathbf{P}\mathbf{B}) \quad (18)$$

Due to the low magnitude of the relative accelerations that are attainable at LEO, this activation strategy is applied every 10 min. This allows for lower frequencies

of actuation and for the drag forces to have enough time to change the orbits of the spacecraft. Note that all the components in the above activation strategy would be available in real time onboard the spacecraft.

#### 4.2. Critical value for the magnitude of differential drag acceleration

As it can be seen in Eqs. (12) and (13), the control signal  $\hat{u}$  is only present in one of the three elements constituting  $\dot{V}$ . Consequently, this element, namely the product  $\beta\hat{u}$ , is the only one that can be used to influence the behavior of  $\dot{V}$  which must be always negative to insure that the system is stable in the sense of Lyapunov. This suggests that there must be a minimum value for  $a_{Drel}$  that allows for  $\dot{V}$  to be negative for given values of  $\beta$  and  $\delta$ , since  $a_{Drel}$  influences the magnitude of the product  $\beta\hat{u}$ . This value is found analytically by solving the following inequality:

$$0 \geq \mathbf{e}^T \mathbf{P}\mathbf{B}a_{Drel}\hat{u} - \delta \quad (19)$$

which results from the inequality  $\Delta \leq 0$ . Solving this expression for  $a_{Drel}$  yields:

$$a_{Drel} \geq \frac{\delta}{|\mathbf{e}^T \mathbf{P}\mathbf{B}|} \quad (20)$$

The absolute value comes from replacing the  $\hat{u}$  for  $-\text{sign}(\mathbf{e}^T \mathbf{P}\mathbf{B})$ . This inequality indicates that if the differential drag acceleration between the spacecraft is larger than the right hand side of the inequality, the derivative of the Lyapunov function will be negative, and consequently the tracking error will go to zero. The right hand side of the inequality then constitutes an analytical critical value for the magnitude of the differential drag, which can be calculated in real time during the maneuver, and it provides a proxy value for the necessary atmospheric density to ensure stability for the controller. This lower bound or critical value is defined as:

$$a_{Dcrit} = \frac{\delta}{|\mathbf{e}^T \mathbf{P}\mathbf{B}|} = \frac{\mathbf{e}^T \mathbf{P}(\mathbf{A}_d \mathbf{x} - \mathbf{f}(\mathbf{x}) + \mathbf{B}\mathbf{u}_d)}{|\mathbf{e}^T \mathbf{P}\mathbf{B}|} \quad (21)$$

For the simplest case in which the controller acts as a regulator (see Eq. (17)) Eq. (21) becomes:

$$a_{Dcrit} = \frac{\mathbf{e}^T \mathbf{P}\mathbf{f}(\mathbf{x})}{|\mathbf{e}^T \mathbf{P}\mathbf{B}|} \quad (22)$$

As it can be observed from Eq. (22), the critical  $a_{Dcrit}$  depends on the tracking error vector  $\mathbf{e}$  and the matrices  $\mathbf{P}$  and  $\mathbf{B}$  for the cases in which the nonlinear system is directly tracking the desired guidance or being regulated.  $\mathbf{B}$ , and  $\mathbf{e}$  cannot be changed by design; however, the matrix  $\mathbf{P}$ , (determined in Eq. (11)) depends only on the matrices  $\mathbf{Q}$ , and  $\mathbf{A}_d$ , which are chosen provided that they satisfy some requisites, namely,  $\mathbf{Q}$  being symmetric positive definite and  $\mathbf{A}_d$  being Hurwitz and being an approximation of the system dynamics.

#### 4.3. Matrix derivatives

Choosing appropriate values for the entries of  $\mathbf{Q}$  and  $\mathbf{A}_d$  will unequivocally modify the behavior of  $a_{Dcrit}$ . To gain a

better understanding of the relationship between the entries of matrices  $\underline{Q}$  and  $\underline{A}_d$  and  $a_{Dcrit}$ , the partial derivatives of  $a_{Dcrit}$  in terms of the matrices  $\underline{Q}$ , and  $\underline{A}_d$  are calculated.

The development of these partial derivatives requires the definition the following four matrix derivative representations defined in Ref. [16] (Eqs. (23), (26)–(28)):

$$\frac{\partial \underline{Y}}{\partial \underline{X}} = \underline{Y}, \quad \underline{X} = \begin{bmatrix} (\underline{Y}, X_{11}) & \cdots & (\underline{Y}, X_{1n}) \\ \vdots & \ddots & \vdots \\ (\underline{Y}, X_{n1}) & \cdots & (\underline{Y}, X_{nn}) \end{bmatrix} \quad (23)$$

Eq. (23) shows the general representation for the partial derivative of an  $n$ -by- $n$  matrix  $\underline{Y}$  in terms of the  $n$ -by- $n$  matrix  $\underline{X}$ .

A very useful operator when dealing with matrix derivatives is the  $vec$  operator which for an  $n$ -by- $n$   $\underline{Z}$  matrix is defined in Ref. [16] as:

$$vec(\underline{Z}) = \underline{Z}_v = [Z_{11} \ \cdots \ Z_{n1} \ \cdots \ Z_{1n} \ \cdots \ Z_{nn}]^T \quad (24)$$

Its inverse operator is defined as:

$$unvec(\underline{Z}_v) = \underline{Z} = \begin{bmatrix} Z_{11} & \cdots & Z_{1n} \\ \vdots & \ddots & \vdots \\ Z_{n1} & \cdots & Z_{nn} \end{bmatrix} \quad (25)$$

The following different representations of the general matrix derivative can be used for finding complicated derivatives (matrix derivative chain rule, matrix derivative product rule, etc.):

$$\frac{\partial \underline{Y}_v}{\partial \underline{X}_v} = vec(\underline{Y}), vec(\underline{X}) = \begin{bmatrix} (vec(\underline{Y}))^T, X_{11} \\ \vdots \\ (vec(\underline{Y}))^T, X_{n1} \\ \vdots \\ (vec(\underline{Y}))^T, X_{1n} \\ \vdots \\ (vec(\underline{Y}))^T, X_{nn} \end{bmatrix} \quad (26)$$

$$\frac{\partial \underline{Y}_v}{\partial \underline{X}} = vec(\underline{Y}), \underline{X} = \begin{bmatrix} (vec(\underline{Y}), X_{11}) & \cdots & (vec(\underline{Y}), X_{1n}) \\ \vdots & \ddots & \vdots \\ (vec(\underline{Y}), X_{n1}) & \cdots & (vec(\underline{Y}), X_{nn}) \end{bmatrix} \quad (27)$$

$$\frac{\partial [Y_v]^T}{\partial \underline{X}} = [vec(\underline{Y})]^T, \underline{X} = \begin{bmatrix} ([vec(\underline{Y})]^T, X_{11}) & \cdots & ([vec(\underline{Y})]^T, X_{1n}) \\ \vdots & \ddots & \vdots \\ ([vec(\underline{Y})]^T, X_{n1}) & \cdots & ([vec(\underline{Y})]^T, X_{nn}) \end{bmatrix} \quad (28)$$

where the vectors  $\underline{Y}_v$  and  $\underline{X}_v$  are the vectorized ( $vec$ ) versions of the matrices  $\underline{Y}$  and  $\underline{X}$ . By observing the representations in Eqs. (26)–(28), it is readily concluded that these three matrix derivatives, containing vectorized forms of the matrices  $\underline{X}$  and  $\underline{Y}$ , contain the same entries as the general matrix derivative (Eq. (23)), but organized in different structures. By rearranging the entries in these

three matrix derivatives, it is possible to obtain the original matrix derivative.

Three reversible transformations from the representations in Eqs. (26)–(28) to the general matrix derivative representation in Eq. (23) are defined as follows:

- Transformation 1:

$$\frac{\partial \underline{Y}}{\partial \underline{X}} = T_1 \left( \frac{\partial \underline{Y}_v}{\partial \underline{X}_v} \right) \quad (29)$$

Input:  $n^2$ -by- $n^2$  matrix  $\underline{Y}_v, \underline{X}_v$ .

Output:  $n^2$ -by- $n^2$  matrix  $\underline{Y}, \underline{X}$ .

Transpose each of the rows of the input matrix  $\underline{Y}_v, \underline{X}_v$  to obtain  $n$  vectors.

Unvectorize each one of these  $n$  vectors to obtain  $n$   $n$ -by- $n$  sub-matrices.

These sub-matrices are the blocks that form the output matrix  $\underline{Y}, \underline{X}$ .

- Inverse Transformation 1:

$$\frac{\partial \underline{Y}_v}{\partial \underline{X}_v} = T_1^{-1} \left( \frac{\partial \underline{Y}}{\partial \underline{X}} \right) \quad (30)$$

Input:  $n^2$ -by- $n^2$  matrix  $\underline{Y}, \underline{X}$ .

Output:  $n^2$ -by- $n^2$  matrix  $\underline{Y}_v, \underline{X}_v$ .

Divide the input matrix  $\underline{Y}, \underline{X}$  into  $n$  blocks, each composed of one  $n$ -by- $n$  sub-matrix.

Vectorize all of these sub-matrices to form  $n$  vectors.

These vectors are rows of the  $n^2$ -by- $n^2$  matrix  $\underline{Y}_v, \underline{X}_v$ .

- Transformation 2:

$$\frac{\partial \underline{Y}}{\partial \underline{X}} = T_2 \left( \frac{\partial \underline{Y}_v}{\partial \underline{X}} \right) \quad (31)$$

Input:  $n^3$ -by- $n$  matrix  $\underline{Y}_v, \underline{X}$ .

Output:  $n^2$ -by- $n^2$  matrix  $\underline{Y}, \underline{X}$ .

Divide the input matrix  $\underline{Y}_v, \underline{X}$  into  $n$  blocks each composed of an  $n^2$ -by-1 vectors.

Unvectorize each one of these  $n$  vectors to obtain  $n$   $n$ -by- $n$  sub-matrices.

These sub-matrices are the blocks that form the output matrix  $\underline{Y}, \underline{X}$ .

- Inverse Transformation 2:

$$\frac{\partial \underline{Y}_v}{\partial \underline{X}} = T_2^{-1} \left( \frac{\partial \underline{Y}}{\partial \underline{X}} \right) \quad (32)$$

Input:  $n^2$ -by- $n^2$  matrix  $\underline{Y}, \underline{X}$ .

Output:  $n^3$ -by- $n$  matrix  $\underline{Y}_v, \underline{X}$ .

Divide the input matrix  $\underline{Y}, \underline{X}$  into  $n$  blocks, each composed of an  $n$ -by- $n$  sub-matrix.

Vectorize all of these sub-matrices to form  $n$  vectors  $n^2$ -by-1.

These  $n^2$ -by-1 vectors are the blocks that form the  $n^3$ -by- $n$  output matrix  $\underline{Y}_v, \underline{X}$ .

- Transformation 3:

$$\frac{\partial \underline{Y}}{\partial \underline{X}} = T_3 \left( \frac{\partial [Y_v]^T}{\partial \underline{X}} \right) \quad (33)$$

Input:  $n^3$ -by- $n$  matrix  $[\mathbf{Y}_v]^T, \mathbf{X}$ .  
 Output:  $n^2$ -by- $n^2$  matrix  $\underline{\mathbf{Y}}\underline{\mathbf{X}}$ .  
 Divide the input matrix  $[\mathbf{Y}_v]^T, \mathbf{X}$  into  $n$  blocks each composed of a 1-by- $n^2$  vectors.  
 Transpose these vectors to obtain  $n^2$ -by-1 vectors.  
 Unvectorize each one of these  $n$  vectors to obtain  $n$   $n$ -by- $n$  sub-matrices.  
 These sub-matrices are the blocks that form the output matrix  $\underline{\mathbf{Y}}\underline{\mathbf{X}}$ .

- Inverse Transformation 3:

$$\frac{\partial[\mathbf{Y}_v]^T}{\partial\mathbf{X}} = T_3^{-1} \left( \frac{\partial\underline{\mathbf{Y}}}{\partial\underline{\mathbf{X}}} \right) \quad (34)$$

Input:  $n^2$ -by- $n^2$  matrix  $\underline{\mathbf{Y}}\underline{\mathbf{X}}$ .  
 Output:  $n$ -by- $n^3$  matrix  $[\mathbf{Y}_v]^T, \mathbf{X}$ .  
 Divide the input matrix  $\underline{\mathbf{Y}}\underline{\mathbf{X}}$  into  $n$  blocks, each composed of a  $n$ -by- $n$  sub-matrices.  
 Vectorize all of these sub-matrices to form  $n$  vectors  $n^2$ -by-1.  
 Transpose these vectors to obtain 1-by- $n^2$  vectors.  
 These 1-by- $n^2$  vectors are the blocks that form the  $n$ -by- $n^3$  output matrix  $[\mathbf{Y}_v]^T, \mathbf{X}$ .

The first step in the development of the desired partial derivatives ( $a_{Dcrit, \underline{\mathbf{Q}}}$  and  $a_{Dcrit, \underline{\mathbf{A}}_d}$ ) is to find the partial derivative of  $a_{Dcrit}$  in terms of the matrix  $\underline{\mathbf{P}}$ . This is accomplished by using Eq. (22) in which  $a_{Dcrit}$  is explicitly expressed in terms of  $\underline{\mathbf{P}}$ .

Eq. (22) can be rewritten as:

$$a_{Dcrit} = \frac{\mathbf{e}^T \underline{\mathbf{P}} \mathbf{f}(\mathbf{x})}{|\mathbf{e}^T \underline{\mathbf{P}} \mathbf{B}|} = \frac{num}{den} \quad (35)$$

The partial derivatives of the numerator and the denominator in terms of the matrix  $\underline{\mathbf{P}}$  are found to be:

$$\frac{\partial num}{\partial \underline{\mathbf{P}}} = \mathbf{e}^T \mathbf{f}(\mathbf{x})^T, \quad \frac{\partial den}{\partial \underline{\mathbf{P}}} = \frac{\mathbf{e}^T \underline{\mathbf{P}} \mathbf{B}}{|\mathbf{e}^T \underline{\mathbf{P}} \mathbf{B}|} \mathbf{e} \mathbf{B}^T \quad (36)$$

After using the derivative quotient rule and some algebra the resulting expression is found:

$$\frac{\partial a_{Dcrit}}{\partial \underline{\mathbf{P}}} = \frac{\mathbf{e}^T \mathbf{f}(\mathbf{x})}{|\mathbf{e}^T \underline{\mathbf{P}} \mathbf{B}|} - \frac{(\mathbf{e}^T \underline{\mathbf{P}} \mathbf{B})(\mathbf{e}^T \mathbf{P} \mathbf{f}(\mathbf{x})) \mathbf{e} \mathbf{B}^T}{|\mathbf{e}^T \underline{\mathbf{P}} \mathbf{B}|^3} \quad (37)$$

The second step is to obtain the partial derivatives of the matrix  $\underline{\mathbf{P}}$  in terms of the matrices  $\underline{\mathbf{Q}}$ , and  $\underline{\mathbf{A}}_d$ . To obtain these derivatives Eq. (11) is rewritten as:

$$\begin{aligned} \underline{\mathbf{A}}_v \mathbf{P}_v &= -\underline{\mathbf{Q}}_v, \\ \underline{\mathbf{A}}_v &= \mathbf{I}_{4 \times 4} \otimes \underline{\mathbf{A}}_d + \underline{\mathbf{A}}_d \otimes \mathbf{I}_{4 \times 4}, \quad \mathbf{P}_v = \text{vec}(\underline{\mathbf{P}}), \quad \underline{\mathbf{Q}}_v = \text{vec}(\underline{\mathbf{Q}}) \end{aligned} \quad (38)$$

where  $\otimes$  represent the Kronecker product defined in Ref. [16] for the same  $n$ -by- $n$   $\underline{\mathbf{Y}}$  and  $\underline{\mathbf{X}}$  matrices as:

$$\underline{\mathbf{X}} \otimes \underline{\mathbf{Y}} = \begin{bmatrix} (X_{11} \underline{\mathbf{Y}}) & \cdots & (X_{1n} \underline{\mathbf{Y}}) \\ \vdots & \ddots & \vdots \\ (X_{n1} \underline{\mathbf{Y}}) & \cdots & (X_{nn} \underline{\mathbf{Y}}) \end{bmatrix} \quad (39)$$

The transformation in Eq. (38) (found in Ref. [16]) allows for the formulation of an explicit equation of the elements of the matrix  $\underline{\mathbf{P}}$  in terms of the elements of the

matrices  $\underline{\mathbf{Q}}$ , and  $\underline{\mathbf{A}}_d$ , which is found to be:

$$\mathbf{P}_v = -\underline{\mathbf{A}}_v^{-1} \underline{\mathbf{Q}}_v \quad (40)$$

Using Eq. (40) it is possible to find the partial derivatives of the vector  $\mathbf{P}_v$  in terms of the vector  $\underline{\mathbf{Q}}_v$ :

$$\frac{\partial \mathbf{P}_v}{\partial \underline{\mathbf{Q}}_v} = \left( -\underline{\mathbf{A}}_v^{-1} \right)^T \quad (41)$$

Subsequently, Transformation 1 is used to obtain the partial derivative of the matrix  $\underline{\mathbf{P}}$  in terms of the matrix  $\underline{\mathbf{Q}}$ , which yields:

$$\frac{\partial \underline{\mathbf{P}}}{\partial \underline{\mathbf{Q}}} = T_1 \left( \left( -\underline{\mathbf{A}}_v^{-1} \right)^T \right) \quad (42)$$

Again, using Eq. (40) it is possible to find the partial derivatives of the vector  $\mathbf{P}_v$  in terms of the matrix  $\underline{\mathbf{A}}_v$ :

$$\frac{\partial \mathbf{P}_v}{\partial \underline{\mathbf{A}}_v} = \left( \mathbf{I}_{16 \times 16} \otimes \underline{\mathbf{A}}_v^{-1} \right) \underline{\mathbf{U}}_{16 \times 16} \left( \mathbf{I}_{16 \times 16} \otimes \underline{\mathbf{A}}_v^{-1} \right) \left( \mathbf{I}_{16 \times 16} \otimes \underline{\mathbf{Q}}_v \right) \quad (43)$$

where  $\underline{\mathbf{U}}_{n \times n}$  is an  $n$ -by- $n$  permutation matrix defined as:

$$\underline{\mathbf{U}}_{n \times n} = \sum_r \sum_s^n \mathbf{E}_{rs} \otimes \mathbf{E}_{rs} \quad (44)$$

where the matrix  $\mathbf{E}_{rs}$  is an elementary matrix with a one at position  $r, s$  and zeros elsewhere. Afterwards, the derivative of  $\underline{\mathbf{A}}_v$  in terms of  $\underline{\mathbf{A}}_d$  is found to be:

$$\frac{\partial \underline{\mathbf{A}}_v}{\partial \underline{\mathbf{A}}_d} = \left( \mathbf{I}_{4 \times 4} \otimes \underline{\mathbf{U}}_1 \right) \left( \underline{\mathbf{U}}_{4 \times 4} \otimes \mathbf{I}_{4 \times 4} \right) \left( \mathbf{I}_{4 \times 4} \otimes \underline{\mathbf{U}}_1 \right) + \underline{\mathbf{U}}_{4 \times 4} \otimes \mathbf{I}_{4 \times 4} \quad (45)$$

where  $\underline{\mathbf{U}}_1$  is a permutation matrix defined as:

$$\underline{\mathbf{U}}_1 = \sum_r \sum_s^4 \mathbf{E}_{rs} \otimes \mathbf{E}_{rs}^T \quad (46)$$

The matrix chain rule, as defined by Ref. [16], is used to obtain the partial derivative of  $\mathbf{P}_v$  in terms of the matrix  $\underline{\mathbf{A}}_d$ :

$$\frac{\partial \mathbf{P}_v}{\partial \underline{\mathbf{A}}_d} = \left[ \frac{\partial [\text{vec}(\underline{\mathbf{A}}_v)]^T}{\partial \underline{\mathbf{A}}_d} \otimes \mathbf{I}_{16 \times 16} \right] \left[ \mathbf{I}_{4 \times 4} \otimes \frac{\partial \mathbf{P}_v}{\partial \text{vec}(\underline{\mathbf{A}}_v)} \right] \quad (47)$$

Using inverse Transformation 1, inverse transformation 3, and Eqs. (45) and (43) the results of Eq. (47) become:

$$\frac{\partial \mathbf{P}_v}{\partial \underline{\mathbf{A}}_d} = \left[ T_3^{-1} \left( \frac{\partial \underline{\mathbf{A}}_v}{\partial \underline{\mathbf{A}}_d} \right) \otimes \mathbf{I}_{16 \times 16} \right] \left[ \mathbf{I}_{4 \times 4} \otimes T_1^{-1} \left( \frac{\partial \mathbf{P}_v}{\partial \underline{\mathbf{A}}_v} \right) \right] \quad (48)$$

Transformation 2 is used to obtain the partial derivative of the matrix  $\underline{\mathbf{P}}$  in terms of the matrix  $\underline{\mathbf{A}}_d$ , which yields:

$$\frac{\partial \underline{\mathbf{P}}}{\partial \underline{\mathbf{A}}_d} = T_2 \left( \frac{\partial \mathbf{P}_v}{\partial \underline{\mathbf{A}}_d} \right) \quad (49)$$

Next, the matrix chain rule is used again to obtain the partial derivative of the scalar  $a_{Dcrit}$  in terms of the matrix  $\underline{\mathbf{Q}}$ :

$$\frac{\partial a_{Dcrit}}{\partial \underline{\mathbf{Q}}} = \left[ \frac{\partial [\text{vec}(\underline{\mathbf{P}})]^T}{\partial \underline{\mathbf{Q}}} \otimes \mathbf{I}_{1 \times 1} \right] \left[ \mathbf{I}_{4 \times 4} \otimes \frac{\partial a_{Dcrit}}{\partial \text{vec}(\underline{\mathbf{P}})} \right] \quad (50)$$

Using inverse Transformation 1, inverse Transformation 3 and Eqs. (42) and (37) the results of Eq. (50)

become:

$$\frac{\partial a_{Dcrit}}{\partial \underline{Q}} = T_3^{-1} \left( \frac{\partial \underline{P}}{\partial \underline{Q}} \right) \left[ \mathbf{I}_{4 \times 4} \otimes T_1^{-1} \left( \frac{\partial a_{Dcrit}}{\partial \underline{P}} \right) \right] \quad (51)$$

Finally, the matrix chain rule is used again to obtain the partial derivative of the scalar  $a_{Dcrit}$  in terms of the matrix  $\underline{A}_d$  :

$$\frac{\partial a_{Dcrit}}{\partial \underline{A}_d} = \left[ \frac{\partial [\text{vec}(\underline{P})]^T}{\partial \underline{A}_d} \otimes \mathbf{I}_{1 \times 1} \right] \left[ \mathbf{I}_{4 \times 4} \otimes \frac{\partial a_{Dcrit}}{\partial \text{vec}(\underline{P})} \right] \quad (52)$$

Using inverse transformation 1, inverse transformation 3 and Eqs. (49) and (37) the results of Eq. (52) become:

$$\frac{\partial a_{Dcrit}}{\partial \underline{A}_d} = T_3^{-1} \left( \frac{\partial \underline{P}}{\partial \underline{A}_d} \right) \left[ \mathbf{I}_{4 \times 4} \otimes T_1^{-1} \left( \frac{\partial a_{Dcrit}}{\partial \underline{P}} \right) \right] \quad (53)$$

Eqs. (51) and (53) provide analytical expressions that can be calculated in real time, describing the behavior of  $a_{Dcrit}$  in terms of each and every one of the entries of the matrices  $\underline{Q}$  and  $\underline{A}_d$ , which can be changed provided that they satisfy their restrictions.

### 5. Adaptive Lyapunov control strategy

By calculating the partial derivatives defined in Eqs. (51) and (53), the entries of the matrices  $\underline{Q}$  and  $\underline{A}_d$ , to which  $a_{Dcrit}$  is the most sensitive are identified (those entries which have the largest partial derivative). Once these entries are identified, the one with the highest partial derivative is selected, and slightly modified by a small value ( $\delta_A = 10^{-6}$  for  $\underline{A}_d$ , and  $\delta_Q = 10^{-6}$  for  $\underline{Q}$ ). The sign of this modification is chosen such that it reduces the derivative of  $a_{Dcrit}$ , thus inducing a downward trend in the behavior of the critical value for the magnitude of the differential acceleration. By reducing this critical value the overall robustness of the controller is improved. The adaptive variations in the  $\underline{Q}$  and  $\underline{A}_d$  are expressed as:

$$\frac{dA_{ij}}{dt} = \kappa_A \left[ -\text{sign} \left( \frac{\partial a_{Dcrit}}{\partial A_{ij}} \right) \delta_A \right], \quad \frac{dQ_{ij}}{dt} = \kappa_Q \left[ -\text{sign} \left( \frac{\partial a_{Dcrit}}{\partial Q_{ij}} \right) \delta_Q \right] \quad (54)$$

where  $\kappa_A$  and  $\kappa_Q$  are defined as:

$$\kappa_A = \begin{cases} 1 & \text{if } \left| \frac{\partial a_{Dcrit}}{\partial A_{ij}} \right| > \left| \frac{\partial a_{Dcrit}}{\partial A_{kl}} \right| \text{ for } i,j \neq k,l \\ 0 & \text{else} \end{cases}, \quad \kappa_Q = \begin{cases} 1 & \text{if } \left| \frac{\partial a_{Dcrit}}{\partial Q_{ij}} \right| > \left| \frac{\partial a_{Dcrit}}{\partial Q_{kl}} \right| \text{ for } i,j \neq k,l \\ 0 & \text{else} \end{cases} \quad (55)$$

These were designed such that the modified  $\underline{Q}$  and  $\underline{A}_d$  matrices still satisfy their requirements of positive definiteness and symmetry for  $\underline{Q}$  and for  $\underline{A}_d$  being Hurwitz. The adaptations of the  $\underline{Q}$  and  $\underline{A}_d$  matrices also affect the panels' activation strategy since they cause variations in  $\underline{P}$  which is used for the panel activation strategy (see Eq. (18)). In other words, the adaptations of the matrices  $\underline{Q}$  and  $\underline{A}_d$  result in an adaptation of the quadratic Lyapunov function shown in Eq. (9). The adaptations are applied at the same time that the drag panels' activation strategy is applied, that is every 10 min. The control strategy is summarized in Fig. 2.

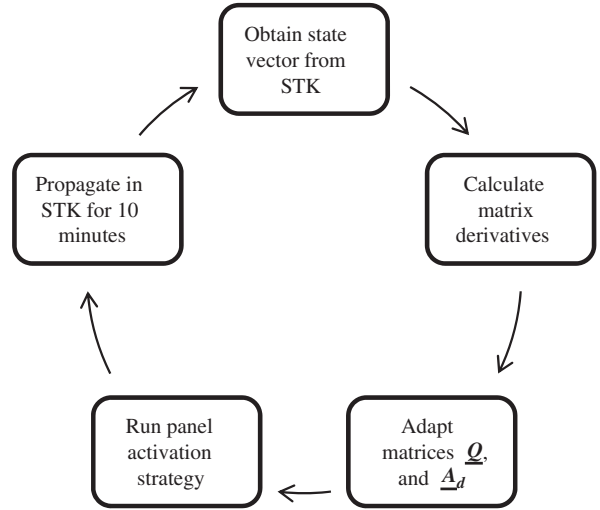


Fig. 2. Control strategy diagram.

### 6. Numerical simulations

The proposed technique was validated using computer numerical simulations. The initial orbital elements of the target and other parameters for the numerical simulations are shown in Table 1. The target and chaser spacecraft are assumed to be identical, therefore drag coefficient and frontal areas for all panel configurations are the same. The initial relative position and velocity of the chaser in the LVLH frame are shown in Table 2 (the same initial state was used in previous work in Ref. [9]).

An STK scenario with full gravitational field model, variable atmospheric density (using NRLMSISE-00 available in STK) and solar pressure radiation effects is used. STK's high-precision orbit propagator (HPOP) is used for simulating the maneuvers. The control strategy is implemented in MATLAB, which interacts with the STK scenario using STK Connect commands. The nonlinear dynamics of the system in the inertial frame are propagated in STK. At each time step, STK sends the state variables to MATLAB where they are transformed into the LVLH frame. The partial derivatives of  $a_{Dcrit}$ , in terms of the matrices  $\underline{Q}$  and  $\underline{A}_d$  are computed (see Eqs. (51) and (53)), and the adaptation of these matrices is performed (see Eq. (54)). This allows for the recalculation of the matrix  $\underline{P}$  and the calculation of the control signal. This signal is fed into STK in the form of panel configurations for the spacecraft. To reduce the frequency of actuation and allow the drag forces enough time to change the orbits, the adaptive Lyapunov controller was activated every 10 min. Moreover, the rendezvous maneuver was assumed to be finalized when the inter spacecraft distance was below 10 m.

Noteworthy, both the adaptive Lyapunov approach here developed, as well as the non adaptive Lyapunov approach suggested earlier by the authors ([9]), are able to drive the spacecraft to relative distances in the order of a few meters, with no propellant required, outperforming by orders of magnitude the results presented in Ref. [18].

Simulations of the adaptive Lyapunov controller are compared with simulations of the non adaptive Lyapunov controller presented by the authors in Ref. [9]. The results

**Table 1**  
Simulation parameters.

Parameter	Value
Second zonal harmonic $J_2$	$1.08 \times 10^{-3}$ (from Ref. [17])
Mean radius of the Earth $R$ (km)	6378.1363
Earth's gravitational parameter $\mu$ ( $\text{km}^3/\text{s}^2$ )	398600.4418
Target's inclination (deg)	98
Target's semi-major axis (km)	6778
Target's right ascension of the ascending node (deg)	262
Target's argument of perigee (deg)	30
Target's true anomaly (deg)	25
Target's eccentricity	0
$v_s$ (km/s)	7.68
$m$ (kg)	10
$S_{\min}$ ( $\text{m}^2$ )	0.5
$S_0$ ( $\text{m}^2$ )	1.3
$S_{\max}$ ( $\text{m}^2$ )	2.5
$C_{D\min}$	1.5
$C_{D0}$	2
$C_{D\max}$	2.5

**Table 2**  
Initial conditions in the LVLH frame.

Parameter	Value
$x$ (km)	-1
$y$ (km)	-2
$\dot{x}$ (km/s)	4.8E-007
$\dot{y}$ (km/s)	1.70E-04

of the simulations are presented in Figs. 3–7, comparing the maneuver trajectories, control sequences, critical values for the magnitude of the differential acceleration, and errors between the non-adaptive Lyapunov controller and the adaptive Lyapunov controller.

The adaptive Lyapunov controller was able to reach the rendezvous state after 29 h, which represent a reduction on the maneuver duration of 24% over the non adaptive Lyapunov controller (which took 38 h). Furthermore, the adaptive Lyapunov controller required 56 changes in the panels' configurations, which signifies a reduction on the control effort of 50% over the non adaptive Lyapunov controller (which needed 113). The average value for the critical value for the magnitude of the differential acceleration (shown in Fig. 5) for the adaptive Lyapunov controller was  $4.43 \times 10^{-5} \text{ m/s}^2$ , which means a reduction on this value of 39% over the non adaptive Lyapunov controller (which had  $7.36 \times 10^{-5} \text{ m/s}^2$ ). A reduction in the critical value implies increased margin on control authority during the maneuver.

The non adaptive Lyapunov controller needs more time and a higher control effort since it approaches the rendezvous state performing more persistent and higher oscillations (these oscillations can be seen in Fig. 7, after 6 h have elapsed, and in Fig. 3(right)). The reduction on the maneuver time and the control effort is caused by the adaptation of the matrix  $\underline{P}$  which allows the adaptive Lyapunov control to tune itself as the error evolves; this results in lower oscillations on the errors behavior (see Fig. 7) and in the trajectory itself (see Fig. 3(right) in the later stages of the maneuver, which is when smoother/finer action is required.

Fig. 7(right) also shows an increase of the error during the first portion of the maneuver, which also means an

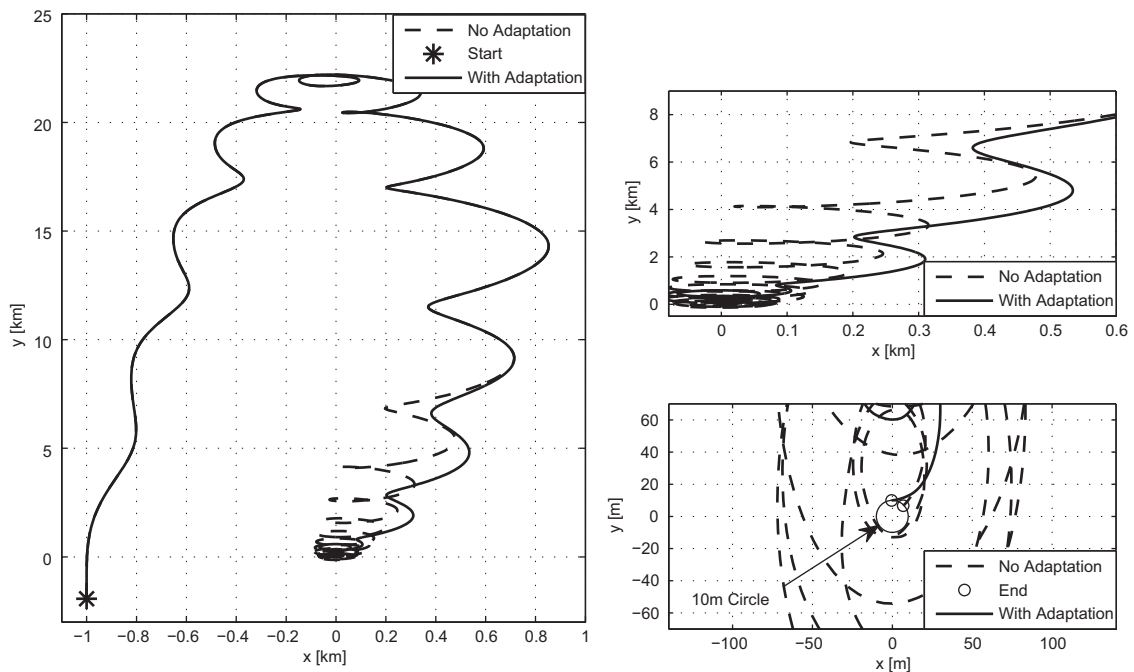


**Fig. 3.** Trajectory in the  $x$ - $y$  plane: (left) complete maneuver, (right top, and bottom) final stages of the maneuver.

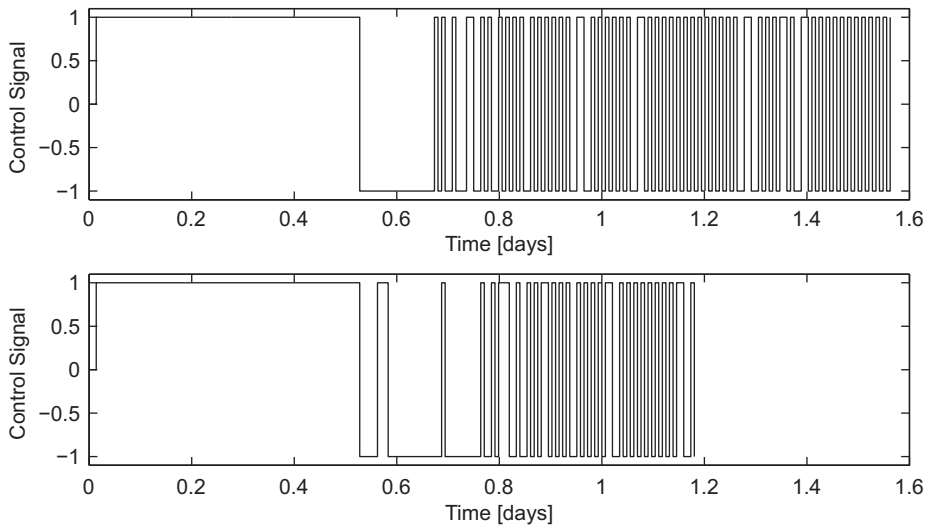


Fig. 4. Control signals: (top) non-adaptive Lyapunov controller, (bottom) adaptive Lyapunov controller.

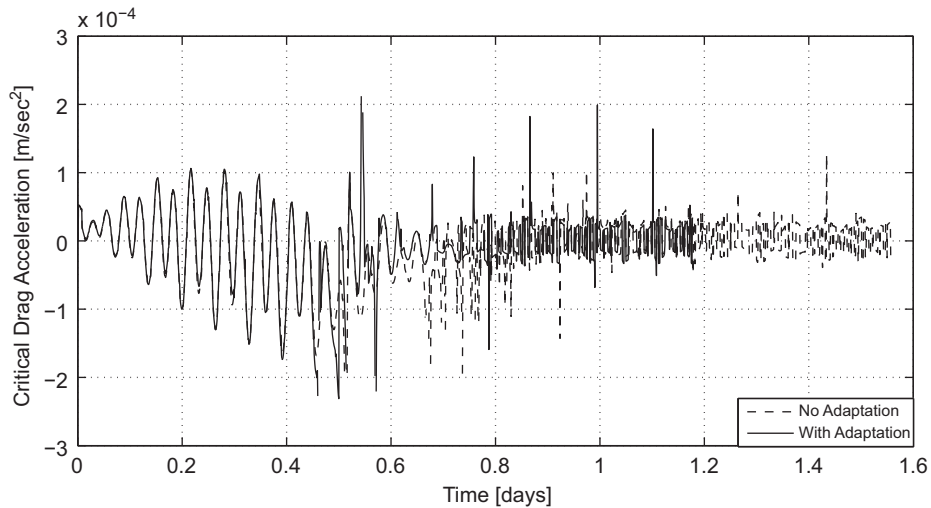
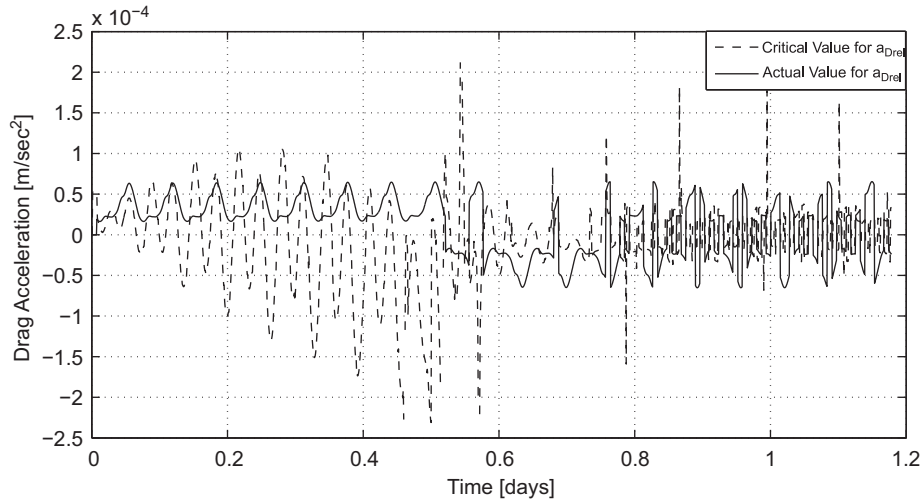


Fig. 5. Critical value for the magnitude of the differential acceleration ( $a_{crit}$ ) over the entire maneuver.

increase of the Lyapunov function, before the system can finally drive itself towards the zero error desired state. This is due to two main factors. The first reason is that the control is allowed to change state only every 10 min, ignoring required changes in the panels configurations within that time frame. This was imposed to enable realistic simulations, and remove the possibility of chattering. In addition, despite the average reduction of the differential drag critical value obtained with the adaptive Lyapunov controller, there are still intervals where the actual differential drag acceleration is lower than the critical acceleration (see Fig. 6). Overall, the proposed approach still enables rendezvous maneuvers that are realistic from the actuation point of view, in terms of duration, and it holds a potential for straightforward implementation on real spacecraft.

### 7. Conclusions

In this work a novel adaptive Lyapunov controller for spacecraft autonomous rendezvous maneuvers using atmospheric differential drag is presented. An analytical expression for the critical value for the magnitude of the differential acceleration that ensures stability in the sense of Lyapunov for the system is found. Based on this, analytical expressions for the partial derivatives of the critical value with respect to the independent variable matrices required by the Lyapunov controller are derived. These partial derivatives are used for the development of the adaptation strategy for the Lyapunov function. The quadratic Lyapunov function is modified in real time, during flight, minimizing the value of the differential drag critical acceleration, thus maximizing the control authority



**Fig. 6.** Comparison between the critical value for the magnitude of the differential acceleration ( $a_{Dcrit}$ ) and the actual value of the differential acceleration for the adaptive controller.

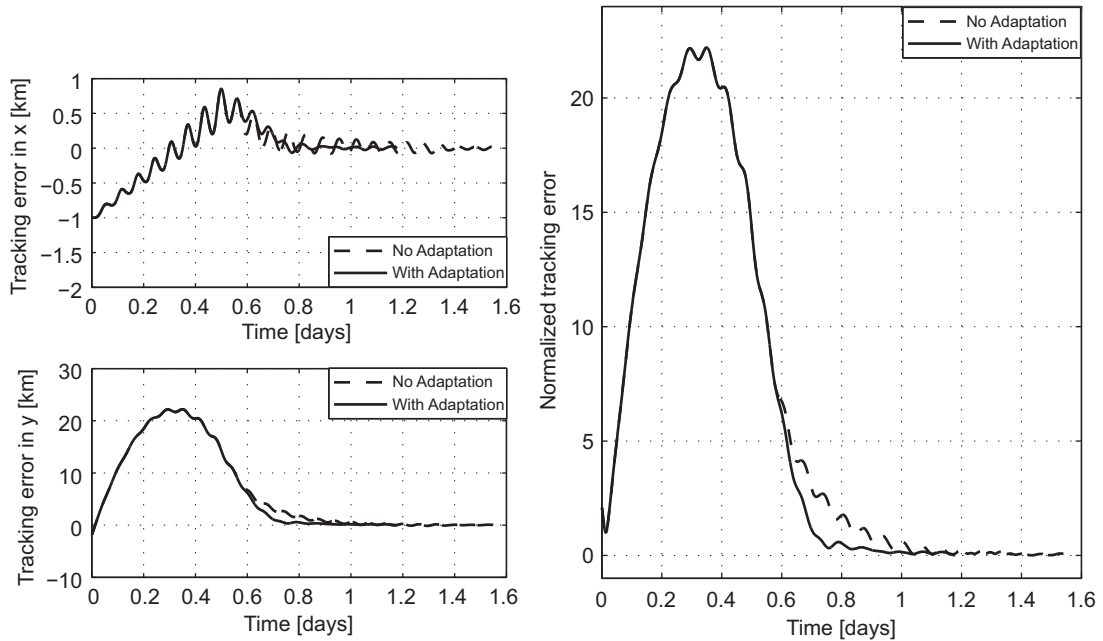


**Fig. 7.** Error over the entire maneuver: (left top)  $x$  error, (left bottom)  $y$  error, (right) normalized error.

margin. The adaptive control method is validated using numerical simulations in Satellite Tool Kit. The performance of the adaptive control method is assessed in terms of the number of switches in the differential acceleration (control effort), and maneuver duration in comparison with the non adaptive Lyapunov controller.

The resulting behavior of the adaptive Lyapunov controller is an improvement over the non adaptive Lyapunov controller since it presents a significantly lower control effort (50% less actuation) and it takes less time to reach the desired rendezvous state (24% less time). The implementation of the reference model on the adaptive Lyapunov controller (in this work the system tracked a constant

final state) is expected to allow the method to track a desired path and not only a constant state, opening to the possibility of potentially performing any type of spacecraft relative maneuver (in the orbital plane) using atmospheric differential drag.

### Acknowledgments

The authors wish to acknowledge the United States Air Force Office of Scientific Research (AFOSR) for sponsoring this investigation under the Young Investigator Program (award no. FA9550-12-1-0072).

The authors wish to thank the organizing committee of the 1st International Academy of Astronautics Conference on Dynamics and Control of Space Systems (DyCoSS'2012), held in Porto, Portugal, 19–21 March 2012. This paper was the winner of the best student paper award for the category: spacecraft guidance, navigation, and control.

The authors would also like to thank Professor Fengyan Li from Rensselaer Polytechnic Institute for her valuable suggestions on the mathematical developments presented in this paper.

## References

- [1] C.L. Leonard, W.M. Hollister, E.V. Bergmann, Orbital formation keeping with differential drag, *AIAA J. Guidance, Control, Dyn.* 12 (1) (1989) 108–113, <http://dx.doi.org/10.2514/3.20374>.
- [2] Maclay, C. Tuttle, Satellite station-keeping of the ORBCOMM constellation via active control of atmospheric drag: operations, constraints, and performance, *Adv. Astronaut. Sci.* 120 (Part I) (2005) 763–773. AAS 05-152.
- [3] A. De Ruiter, J. Lee, A. Ng, A fault-tolerant magnetic spin stabilizing controller for the JC2Sat-FF Mission, in: *AIAA Guidance, Navigation and Control Conference and Exhibit*, Honolulu, Hawaii, 18–21 August 2008. AIAA-2008-7486.
- [4] B. Kumar, A. Ng, K. Yoshihara, A. De Ruiter, Differential drag as a means of spacecraft formation control, in: *Proceedings of the 2007 IEEE Aerospace Conference, Big Sky, MT, March 3–10, 2007*.
- [5] C. Lambert, B.S. Kumar, J.F. Hamel, A. Nga, Implementation and performance of formation flying using differential drag, *Acta Astronaut.* 71 (2012) 68–82, <http://dx.doi.org/10.1016/j.actaastro.2011.08.013>.
- [6] J. Brill, (March 11, 2012). About SSCO. <<http://ssco.gsfc.nasa.gov/about.html>>. (Last accessed March 11, 2012.).
- [7] R. Bevilacqua, M. Romano, Rendezvous maneuvers of multiple spacecraft by differential drag under  $J_2$  perturbation, *AIAA J. Guidance, Control, Dyn.* 31 (6) (2008) 1595–1607, <http://dx.doi.org/10.2514/1.36362>.
- [8] F. Curti, M. Romano, R. Bevilacqua, Lyapunov-based thrusters' selection for spacecraft control: analysis and experimentation, *AIAA J. Guidance, Control, Dyn.* 33 (4) (2010) 1143–1160, <http://dx.doi.org/10.2514/1.47296>.
- [9] D. Perez, R. Bevilacqua, Lyapunov-based Spacecraft Rendezvous Maneuvers Using Differential Drag, AIAA-2011-6630 Paper, AIAA Guidance, Dynamics and Control Conference 2011, Portland, OR.
- [10] V.A. Kamenetskiy, Ye.S. Pyatnitskiy, A gradient method for developing Lyapunov functions in problems of absolute stability, *Avtom. Telemekh.* (1) .
- [11] V.A. Kamenetskiy, Ye.S. Pyatnitskiy, An iterative method of Lyapunov function construction for differential inclusions, *Syst. Control Lett.* 8 (5) (1987) 445–451, [http://dx.doi.org/10.1016/0167-6911\(87\)90085-5](http://dx.doi.org/10.1016/0167-6911(87)90085-5).
- [12] E.A. Barbashin, On construction of Lyapunov functions for non-linear systems, in: *Proc. First Congr. IFAK, Moscow, 1961*, pp. 742–751.
- [13] G. Hill, Researches in lunar theory, *Am. J. Math.* 1 (1) (1878) 5–26.
- [14] W.H. Clohessy, R.S. Wiltshire, Terminal guidance system for satellite rendezvous, *J. Aerosp. Sci.* 27 (9) (1960) 653–658.
- [15] S.A. Schweighart, R.J. Sedwick, High-fidelity linearized  $J_2$  model for satellite formation flight, *J. Guidance, Control, Dyn.* 25 (6) (2002) 1073–1080.
- [16] Alexander Graham, *Kronecker Products and Matrix Calculus: With Applications*, Horwood, Chichester, 1981 120–125.
- [17] D.A. Vallado, *Fundamentals of Astrodynamics and Applications*, second ed. Microcosm Press, Hawthorne, 2004 Backcover.
- [18] R. Bevilacqua, J. Hall, S. Romano, M., Multiple spacecraft assembly maneuvers by differential drag and low thrust engines, *Celestial Mech. Dyn. Astron.* 106 (2010) 69–88, <http://dx.doi.org/10.1007/s10569-009-9240-3>.



**David Pérez** is a Ph.D. candidate in the Mechanical Aerospace and Nuclear Engineering Department at the Rensselaer Polytechnic Institute, Troy, New York. He is the lab manager at the Advanced Autonomous Multiple Spacecraft Laboratory. David's main research interests are Guidance, Navigation and Control of autonomous Spacecraft and Robotics. He received his B.Sc. in Mechanical Engineering in 2008 from the St. Cloud State University, St. Cloud, Minnesota and his M.Eng. in Mechanical Engineering in 2009 from the Rensselaer Polytechnic Institute, Troy, New York.



**Dr. Riccardo Bevilacqua** is an Assistant Professor of the Mechanical, Aerospace, and Nuclear Engineering Department, at Rensselaer Polytechnic Institute. He holds a M.Sc. in Aerospace Engineering (2002), and a Ph. D. in Applied Mathematics (2007), both earned at the University of Rome, "Sapienza", Italy. He was a US National Research Council Post-Doctoral Fellow from 2007 to 2010, before joining RPI. He also worked as project engineer in Mission Analysis at Grupo Mecanica del Vuelo, in Madrid, Spain, during 2003. Dr. Bevilacqua's research interests focus on Guidance, Navigation, and Control of multiple spacecraft systems and multiple robot systems.